Technical University of Denmark

DTU

Feasibility of using ammonia-water mixture in high temperature concentrated solar power plants with direct vapour generation

Modi, Anish; Knudsen, Thomas; Haglind, Fredrik; Clausen, Lasse Røngaard

DTU Library
Technical Information Center of Denmark

Feasibility of using ammonia-water mixture in high temperature concentrated solar power plants with direct vapour generation

Anish Modi*, Thomas Knudsen, Fredrik Haglind, Lasse Røngaard Clausen

Department of Mechanical Engineering, Technical University of Denmark, Nils Koppels Allé, Building 403, DK-2800 Kgs. Lyngby, Denmark

Abstract

Concentrated solar power plants have attracted an increasing interest in the past few years – both with respect to the design of various plant components, and extending the operation hours by employing different types of storage systems. One approach to improve the overall plant performance is to use direct vapour generation with water/steam as both the heat transfer fluid in the solar receivers and the cycle working fluid. This enables to operate the plant with higher turbine inlet temperatures. Available literature suggests that it is feasible to use ammonia-water mixture at high temperatures without corroding the equipment by using suitable additives with the mixture. This paper assesses the thermodynamic feasibility of using ammonia-water mixture in high temperature (450 °C) and high pressure (over 100 bar) concentrated solar power plants with direct vapour generation. The following two cases are compared for the analysis: a simple Rankine cycle and an ammonia-water cycle with a separator for varying the ammonia mass fraction within the cycle. Thermodynamic simulations are performed using Aspen Plus and MATLAB, and performances in terms of overall plant efficiency are evaluated. The comparison between the two cycles when operating from a two-tank molten-salt storage system is also presented. The results suggest that the ammonia-water mixtures show a clear advantage while operating from storage but the simple Rankine cycle outperforms the ammonia-water cycle when the heat input is from solar receiver only.

* Corresponding author. Tel.: +45-45251910; fax: +45-45884325.
E-mail address: anmod@mek.dtu.dk

Nomenclature

AWC   Ammonia-water cycle

CSP   Concentrated solar power

DVG   Direct vapour generation

HTF   Heat transfer fluid

ORC   Organic Rankine cycle

PPTD   Pinch point temperature difference

SRC   Simple Rankine cycle

1. Introduction

In recent times, concentrated solar power (CSP) plants have attracted interest as large scale, commercially viable way to generate electricity [1]. In a CSP plant, the heat transfer fluid (HTF) and the working fluid play an important role as the carriers of energy from the collector/receiver to the turbine. This is commonly done in two stages for a plant operating with a Rankine cycle: in the first stage, the HTF (e.g. synthetic oil, molten salt etc.) collects the energy from the incident solar radiation; and in the second stage, the working fluid (water/steam) receives this energy from the HTF and carries it to the steam turbine. The main disadvantage of such two-fluid systems is that the maximum operating temperature of the HTF is limited by the fluid stability concerns (e.g. approximately 400 °C for the synthetic oil), thus resulting in a low turbine inlet temperature and consequently a low cycle efficiency.

Application of the direct vapour generation (DVG) technology in CSP plants presents the prospect of improvement in the overall plant efficiency while simultaneously decreasing the cost of electricity generation [2]. The pressurized steam is generated directly in the receiver and transported to the steam turbine. The advantages of DVG include a considerably higher maximum working temperature and the use of one fluid as both the HTF and the working fluid possibly resulting in a simplified operation. The main disadvantage of using DVG for CSP plants is that it requires a very complex storage system for uninterrupted operation throughout the day [3].

There were a few proposals to incorporate the Kalina cycle or the organic Rankine cycle (ORC) as bottoming cycles for the CSP plants, or to use solar energy directly as source of a heat input to these cycles, but they were mostly related to low or medium temperature applications [4–10]. Chacartegui et al. [11] presented the possibility of using a CO_2 topping cycle along with an ORC bottoming cycle for central receiver power plants. Nag and Gupta [12] performed an exergy analysis of a high temperature Kalina cycle while Dejfors et al. [13] presented an analysis of using ammonia-water power cycles for direct fired cogeneration plants. Knudsen et al. [14] presented the results from simulation and exergy analysis of a Kalina cycle with a turbine inlet temperature of 550 °C when the heat input is from solar receiver, and 480 °C when the heat input is from a molten-salt storage system. The authors varied the heat input to the cycle so as to maintain the turbine inlet conditions while assuming the same mass flow rate for all the cases. This approach is different from the current study where the different cycle configurations were optimised with the same heat input for all the configurations. Other than this, using ammonia-water mixture in the entire cycle (from receiver to generator) for high temperature CSP plant with DVG has not been studied.

There have been discussions regarding the feasibility of using ammonia-water mixtures at high temperatures due to the nitridation effect resulting in corrosion of the equipment. However, the use ammonia-water mixture as a working fluid at high temperature has been successfully demonstrated in Canoga Park with turbine inlet conditions of 515 °C and 110 bar [15]. Moreover, a patent claims the stability of ammonia-water mixtures along with prevention of nitridation for plant operation preferably up to 2000 °F (1093 °C) for temperature and 10000 psia (689.5 bar) for pressure using suitable additives [16].

The current study is aimed at evaluating the thermodynamic feasibility of using ammonia-water mixture as working fluid in a CSP plant with DVG. The motivation behind this study is that the exergy losses during a heat transfer process can be reduced by using a suitable multi-component working fluid which can evaporate or condense at a varying temperature contrary to the constant evaporating or condensing temperature for a pure substance [17]. This paper presents a comparison between a simple Rankine cycle (SRC) and an ammonia-water cycle (AWC) with different ammonia mass fractions and pressures at the turbine inlet; the ammonia mass fraction being defined as the mass of ammonia in the ammonia-water mixture to the total mass of the mixture. Section 2 presents the assumptions and the modelling procedure for the study. Section 3.1 presents the results from the comparison of the cycles based on first law efficiency and other relevant parameters, while section 3.2 presents the results from the comparison of the required molten-salt mass flow rates when the solar receiver is replaced by a molten-salt storage system as the primary source of heat input. Finally, section 4 concludes the paper.

2. Methodology

The layouts of the compared cycles while receiving heat input solely from solar radiation are presented in Fig. 1 (SRC) and Fig. 2 (AWC). With reference to Fig. 1, the superheated steam obtained from the receiver (stream 1) is expanded in the turbine. The low temperature, low pressure steam (stream 2) is then condensed to obtain saturated liquid (stream 3) which is then pumped till the turbine inlet pressure is attained (stream 4).
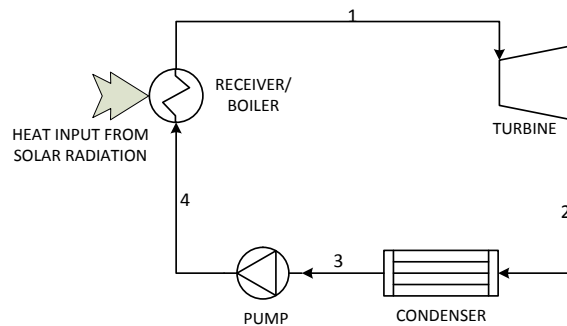
Fig. 1. Schematic of the simple Rankine cycle

Several cycle layouts have been proposed for power plants operating with Kalina cycle or using ammonia-water mixture with different heat sources [17–21]. In this study, the layout was kept in a simple form with one separator and two recuperators as it was compared with the most basic Rankine cycle. With reference to Fig. 2, the working solution ammonia-water mixture entering the turbine (stream 1) is expanded. Energy is recovered from stream 2 to preheat the working solution in recuperator-1. In order to have a low condensation pressure in the condenser-1, a separator is used from which a rich ammonia

vapour (stream 11) and a lean ammonia liquid (stream 12) are obtained. The lean liquid is mixed with the working solution (in mixer-1) and thus the ammonia mass fraction in condenser-1 is reduced. The mass flow rate in the separator loop is determined by the satisfaction of the pinch point criteria for the recuperator-2. A throttle valve is used to bring the pressure of the lean liquid (stream 12) down to the pressure level of working fluid (stream 4) before mixing in mixer-1. The rich vapour (stream 11) is mixed with the basic solution (stream 8) to again form the working fluid (stream 14) before going through the condenser-2 and the pump-2 to increase the pressure equal to the turbine inlet pressure. After the pump-2, the working fluid is heated up to the turbine inlet temperature in the receiver.
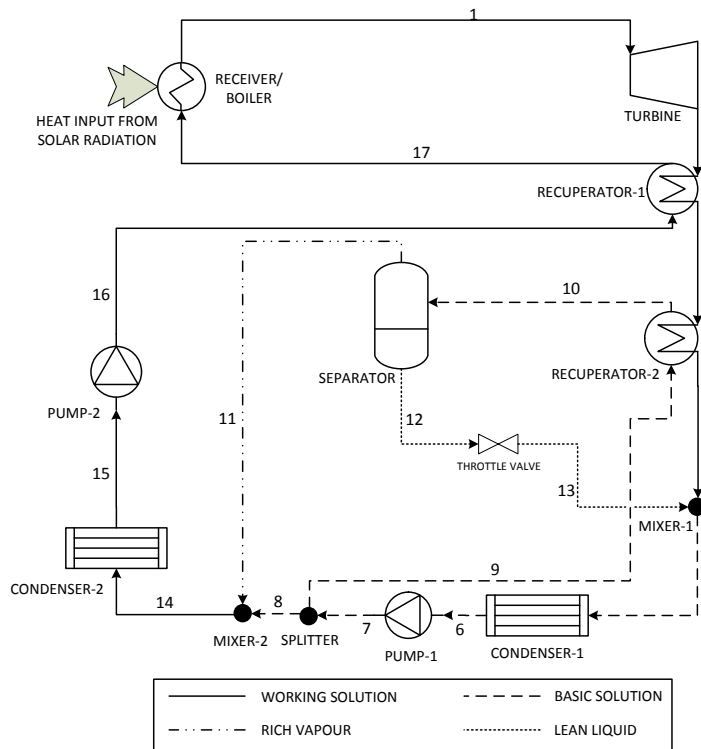

Fig. 2. Schematic of the ammonia-water cycle

The analysis in this paper was divided into the following parts:
1. In the first part, the SRC and the AWC were modelled using Aspen Plus (v7.2) [22]. The thermophysical properties of the working were evaluated using the Peng-Robinson equation of state with Boston-Mathias extension (PR-BM) [23]. All the models were steady-state models. For all the cases, the cycles were optimised to deliver the maximum possible work output while maintaining the pinch point criteria and the same turbine inlet temperature (450 °C). The mass flow rate at the turbine inlet was calculated so as to maintain the receiver/boiler outlet temperature equal to 450 °C. For the SRC, simulations were performed by varying the turbine inlet pressure until the vapour fraction at the turbine outlet reaches its minimum value (0.85). For the AWC, the cycles were optimised by varying the temperature difference between stream 3 and stream 10 (Fig. 2), and the temperature at receiver

inlet (stream 17 in Fig. 2) while maintaining the pinch point criteria. The set of values for various streams for the optimised cycles are also termed as design point operation for the power cycle.

2. In the second part, the solar receiver was replaced by a two-tank molten-salt storage system as the primary source of heat input (Fig. 3) with HITEC molten-salt [24] as the storage medium.
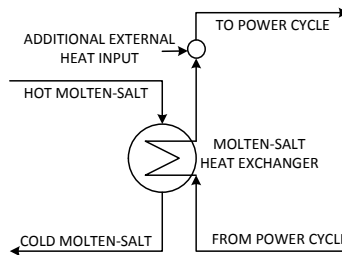

Fig. 3. Two-tank molten-salt storage system with external additional heat input to operate the power cycle at design point

The high temperature of the storage was fixed at 430 °C (assumed 20 °C below the turbine inlet temperature since the storage was supposed to be charged by the vapour generated in the solar receiver itself). Similarly, it was also assumed that the molten-salt can only heat the working fluid up to 410 °C (again 20 °C below the molten-salt hot temperature), and an additional external heater (e.g. a fossil fuel or biomass fired burner) is employed to heat the working fluid to 450 °C, the turbine inlet temperature. The cold temperature of the storage was then calculated so as to maintain the pinch point condition for the storage heat exchanger. It was assumed that the cold temperature of the molten-salt (HITEC) cannot go below 180 °C to avoid freezing of the salt which occurs as 142 °C [24]. The specific heat capacity of HITEC was assumed to be constant and equal to 1567.1 J/kg-K [25]. The molten-salt mass flow rate required by the cycles was then evaluated for different turbine inlet pressures and ammonia mass fractions. Only the discharge cycle for the storage system was considered in the current study. This part of the analysis was modelled using MATLAB (R2013a) as Aspen Plus does not include HITEC as a compound in its database. Also, as MATLAB has a very good interface with REFPROP [26], the thermophysical properties of the working fluid for this part of the analysis were calculated using REFPROP.

The general assumptions for the analysis were as follows:

1. The solar receiver was assumed to be similar to the one used in the PS10 solar power plant for direct steam generation. Similar to the PS10, the efficiency of the receiver was taken as 90.2% (annual average value) and the peak design value of solar irradiance on the receiver as 0.65 MW/m^2 [27]. However, the area of the receiver was assumed to be 42.65 m^2 so that the heat input to the working fluid became 25 MW for all the cases. It was also assumed that the irradiance is evenly distributed over the receiver area. Pressure losses in the receiver were neglected.

2. Pressure drops and heat losses in the other cycle components were neglected.

3. The solar radiation heat input was modelled as a simple heater in Aspen Plus. The recuperators in the AWC were assumed to have a pinch point temperature difference (PPTD) of at least 5 °C. The condensers were assumed to have a PPTD of at least 4 °C. When using the molten-salt storage system instead of the solar receiver for heat input, it was assumed to have a PPTD of minimum 20 °C in the storage heat exchanger. Since a temperature difference of 20 °C between the hot temperature of the molten-salt and the working fluid temperature at the corresponding point in the storage heat exchanger was assumed during both charging and discharging of the storage, a minimum PPTD of

the same value was considered for the entire heat exchanger. All the heat exchangers were modelled as counter-flow heat exchangers.

4. The assumed values of various parameters for the power cycle are mentioned in Table 1.

Table 1. Assumed parameters for the power cycle

Parameter	Assumed value
Turbine inlet temperature	450 °C
Turbine isentropic efficiency	80%
Turbine mechanical efficiency	98%
Pump efficiency (for all pumps)	90%
Minimum allowed vapour fraction at turbine outlet	0.85
Condenser cooling water inlet temperature	20 °C
Condenser cooling water maximum temperature rise	15 °C

3. Results and discussion

The results from the two parts of the analysis, i.e., power cycle optimisation with Aspen Plus and operation with molten-salt storage system using optimised power cycle parameters with MATLAB, are presented below.

3.1. Results from power cycle analysis

The energy available in the solar radiation incident on the receiver surface was calculated by multiplying the design value of the incident solar irradiance with the receiver surface area. It is approximately equal to 27.72 MW. Both the SRC and the AWC were simulated for turbine inlet pressures increasing at an interval of 10 bar between 100 bar and 160 bar. The SRC was however limited to a maximum of 114 bar because of the turbine outlet vapour quality constraint (≥ 0.85). For the AWC, a maximum turbine inlet pressure of 160 bar was achievable without violating the turbine outlet vapour fraction constraint.

The best performing SRC was operating with a turbine inlet pressure of 114 bar and therefore this cycle was used to compare with the performance of the AWC. Fig. 4 shows the variation in the plant efficiency for the AWC at different turbine inlet pressures (between 100 and 160 bar) and ammonia mass fractions (between 0.5 and 0.9). The ammonia mass fractions at turbine inlet were limited in this study to vary between 0.5 and 0.9 as the ammonia mass fractions lower than 0.5 are too close to a Rankine cycle and may not necessarily utilise the sliding evaporation and condensing characteristics of the ammonia-water mixture. For the ammonia mass fractions higher than 0.9, the calculations of the state properties were not always stable and they failed to converge on several occasions.

It may be observed from Fig. 4 that with an increase in the turbine inlet ammonia mass fraction for the AWC, the plant efficiency (which is the ratio of the net work output from the plant to the energy available in the solar radiation incident on the receiver surface) first decreases, reaches a minimum value and then starts to increase again. This behaviour depends on the cycle layout, the amount of recuperation in the cycle and how closely is the pinch point criterion satisfied for various heat exchangers. With increasing turbine inlet ammonia mass fraction, the losses in the condensers, the recuperator-1 and the turbine showed a decreasing trend; whereas the losses in the recuperator-2 first increased and then decreased, depending on the pinch criterion satisfaction and the match between the inlet and the outlet stream

temperature profiles. This, combined with the fact that the losses in the throttle valve and the mixers became negligible at higher turbine inlet mass fractions due to better match in the mixing streams' temperatures, caused the plant efficiency to increase again after a certain value of the turbine inlet ammonia mass fraction.
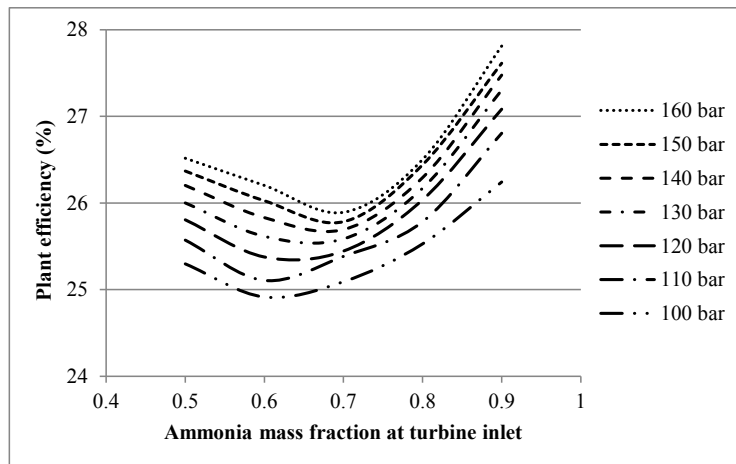

Fig. 4. Cycle efficiency for the AWC at different TIP

Comparing the plant efficiencies for the SRC and the AWC for operation from solar receiver only, it may be observed that the plant efficiency of the AWC with the best performance (27.81% with an ammonia mass fraction of 0.9 and a pressure of 160 bar at the turbine inlet) is slightly lesser than the SRC operating with a turbine inlet pressure of 114 bar (28.19%). Thus, from plant efficiency perspective, the SRC should be the preferred cycle of operation for a CSP plant with heat input from only solar receiver. Though, even in this operation mode (i.e. without storage), there are other benefits of using ammonia-water mixture as the cycle working fluid. The volume flow rate of the working fluid at turbine outlet was much lower for the AWC when compared with the SRC (at the most 14.29 m³/s for the AWC with an ammonia mass fraction of 0.5 and a pressure of 100 bar at turbine inlet as compared to 161.15 m³/s for the SRC with a turbine inlet pressure of 114 bar). It means that the AWC can operate at much higher turbine inlet pressures with a more compact turbine without violating the minimum vapour fraction condition at turbine outlet. This implies a reduction in the turbine cost for the AWC for similar work output as compared to the SRC.

3.2. Results from storage operation analysis

For the SRC operating with a turbine inlet pressure of 114 bar, Fig. 5 shows the temperature vs. heat flow rate or T-Q̇ diagram that was obtained while satisfying the minimum PPTD condition over the heat exchanger. It may be observed from the figure that the molten-salt cannot be operated below a cold temperature of 270 °C for the SRC without violating the pinch point criterion. For the SRC, a molten-salt mass flow rate of 93.28 kg/s was required for operation from storage. Similarly for the AWC, a molten-salt mass flow rate between 61.03 kg/s and 62.19 kg/s was required at a turbine inlet ammonia mass fraction and pressure of 0.9 and 160 bar, and 0.5 and 100 bar respectively. The required molten-salt mass flow rates for all the other cases for the AWC, i.e., between 0.5/100 bar and 0.9/160 bar, were between these two values of molten-salt mass flow rates.
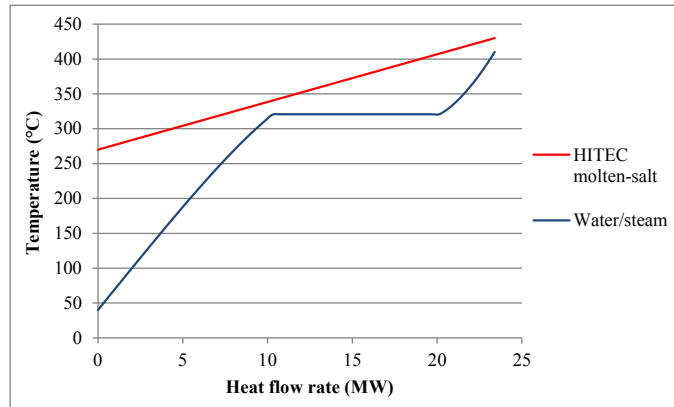
Fig. 5. T-Q̇ diagram for the SRC operating with a turbine inlet pressure of 114 bar
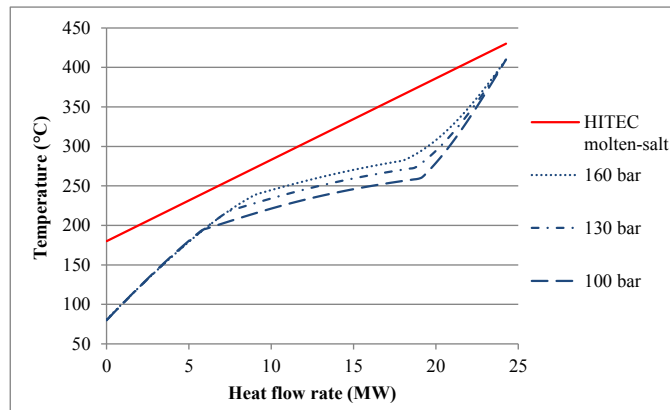

Fig. 6. T-Q̇ diagram for the AWC operating with a turbine inlet ammonia mass fraction of 0.5 at different turbine inlet pressures

Fig. 6 shows the T-Q̇ diagram for a turbine inlet ammonia mass fraction of 0.5 at different turbine inlet pressures. It may be observed that the molten-salt can be used for a much wider range of temperature for ammonia-water mixture as the hot and the cold temperature curves have a better match due to the temperature glide during evaporation. Since the molten-salt mass flow rate was found to be significantly smaller for the AWC, it also means that for a day's operation, the quantity of salt required will be lesser, and therefore also the pumping power and the piping requirements. This makes the AWC an economically better alternative as compared to the SRC when operating from storage. This also makes it possible to use a simple sensible heat storage system instead of the one proposed for DVG operation which is both expensive and complex [3]. It may also be observed that ammonia-water mixture gives a better match with the heat source (molten-salt) with increase in the turbine inlet pressure. Similar observations were made for all the turbine inlet ammonia mass fractions. Comparing Fig. 5 and Fig. 6, it may be noticed that there is a slight difference in the heat input for the SRC and the AWC. This is because two different property calculation methods were used for the two parts of this analysis (i.e. PR-BM for power cycle optimisation and REFPROP for analysis of operation from storage). This however

does not compromise the results of this part of the analysis as the comparison is made with respect to the storage mass flow rate and size, and not for re-optimising the cycle for operation from storage.

The current study analyses the operation from storage once the design point of the power cycle is fixed, and then the cycle is assumed to always operate at that design point. However, in practice, there will be instances when the cycle is being operated in off-design conditions. There is also a mention of an additional external heat input when operating from storage so as to maintain the turbine inlet temperature at the design point. An alternative to this situation could be to operate the cycle in off-design condition with a lower turbine inlet temperature or in sliding pressure mode to avoid having to use a complex storage system [28]. Further work is required to fully analyse the cycle performance in such situations (e.g. an annual performance comparison and optimisation of cycle parameters accordingly) and to assess if using the AWC instead of the SRC is actually beneficial for CSP plants. Thermal energy storage systems are likely to reduce the cost of electricity generation by a significant margin [29], and it is expected that the greater is the share of operation from storage, the more beneficial it becomes to use ammonia-water mixture in the plant instead of water as the working fluid. The same has been concluded by Knudsen et al. [14].

4. Conclusion

Two power cycles, the SRC and the AWC, were modelled and compared as alternatives for CSP plants operating with DVG. The comparison was made by keeping the heat input to the cycle as constant while varying the pressure and the ammonia mass fraction at the turbine inlet. It was observed that when the heat input to the cycle is solely from the solar receiver, the SRC showed a slightly better cycle efficiency than the most promising AWC configuration. However, considering that the volume flow rate at the turbine outlet is significantly lower for the AWC as compared to the SRC, and that the vapour fraction at the turbine outlet is not a limiting factor for the AWC, it allows the AWC to be operated at much higher turbine inlet pressures while using more compact turbines. Another important aspect of a CSP plant is the storage system which is required for a reliable operation and an improved capacity factor. When using a simple two-tank molten-salt storage system with HITEC molten-salt as the storage medium, the AWC showed a clear advantage over the SRC by utilising a wider temperature range, thus significantly reducing the storage size for about the same power output. Using the AWC also makes it possible to use a simplified sensible storage system instead of the complex storage system that is generally proposed for DVG operation. Thus, depending on the annual performance analysis with given solar data and storage requirements, the AWC might prove to be economically more beneficial for CSP plants.

References

[1] Greenpeace International, SolarPACES, and ESTELA, 2009, Concentrating Solar Power: Global Outlook 2009, Amsterdam, The Netherlands.
[2] Zarza E., Valenzuela L., León J., Hennecke K., Eck M., Weyers H.-D., and Eickhoff M., 2004, "Direct steam generation in parabolic troughs: Final results and conclusions of the DISS project," Energy, **29**(5-6), pp. 635–644.
[3] Laing D., Bahl C., Bauer T., Lehmann D., and Steinmann W.-D., 2011, "Thermal energy storage for direct steam generation," Sol. Energy, **85**(4), pp. 627–633.
[4] Lolos P. A., and Rogdakis E. D., 2009, "A Kalina power cycle driven by renewable energy sources," Energy, **34**(4), pp. 457–464.
[5] Mittelman G., and Epstein M., 2010, "A novel power block for CSP systems," Sol. Energy, **84**(10), pp. 1761–1771.
[6] Shankar Ganesh N., and Srinivas T., 2012, "Design and modeling of low temperature solar thermal power station," Appl. Energy, **91**(1), pp. 180–186.
[7] Shankar Ganesh N., and Srinivas T., 2012, "Thermodynamic assessment of heat source arrangements in Kalina power station," J. Energy Eng., **139**(June), pp. 99–108.

[8]   Shankar Ganesh N., and Srinivas T., 2013, "Power augmentation in a Kalina power station for medium temperature low grade heat," J. Sol. Energy Eng., **135**(3), p. 031010.
[9]   Sun F., Ikegami Y., Arima H., and Zhou W., 2013, "Performance analysis of the low-temperature solar-boosted power generation system - Part I: Comparison between Kalina solar system and Rankine solar system," J. Sol. Energy Eng., **135**, p. 011015.
[10]   Sun F., Ikegami Y., Arima H., and Zhou W., 2013, "Performance analysis of the low-temperature solar-boosted power generation system - Part II: Thermodynamic characteristics of the Kalina solar system," J. Sol. Energy Eng., **135**, p. 011006.
[11]   Chacartegui R., Muñoz de Escalona J. M., Sánchez D., Monje B., and Sánchez T., 2011, "Alternative cycles based on carbon dioxide for central receiver solar power plants," Appl. Therm. Eng., **31**(5), pp. 872–879.
[12]   Nag P. K., and Gupta A. V. S. S. K. S., 1998, "Exergy analysis of the Kalina cycle," Appl. Therm. Eng., **18**(6), pp. 427–439.
[13]   Dejfors C., Thorin E., and Svedberg G., 1998, "Ammonia-water power cycles for direct-fired cogeneration applications," Energy Convers. Manag., **39**(16-18), pp. 1675–1681.
[14]   Knudsen T., Clausen L. R., Haglind F., and Modi A., 2013, "Energy and exergy analysis of the Kalina cycle for use in concentrated solar power plants with direct steam generation," Presented at the ISES Solar World Congress 2013. November 3-7, 2013. Cancun, Mexico. To be published in Energy Procedia (Elsevier).
[15]   Mirolli M. D., 2012, "Kalina cycle power systems in waste heat recovery applications," pp. 1–8 [Online]. Available: www.globalcement.com/magazine/articles/721-kalina-cycle-power-systems-in-waste-heat-recovery-applications. [Accessed: 30-Aug-2013].
[16]   Kalina A. I., 2002, Method of preventing nitridation or carburization of metals, United States Patent 6482272 B2.
[17]   Chen H., Goswami D. Y., Rahman M. M., and Stefanakos E. K., 2011, "A supercritical Rankine cycle using zeotropic mixture working fluids for the conversion of low-grade heat into power," Energy, **36**(1), pp. 549–555.
[18]   Ibrahim M. B., and Kovach R. M., 1993, "A Kalina cycle application for power generation," Energy, **18**(9), pp. 961–969.
[19]   Jonsson M., and Yan J., 2001, "Ammonia–water bottoming cycles: a comparison between gas engines and gas diesel engines as prime movers," Energy, **26**(1), pp. 31–44.
[20]   Zhang Y., He M., Jia Z., and Liu X., 2008, "First law-based thermodynamic analysis on Kalina cycle," Front. Energy Power Eng. China, **2**(2), pp. 145–151.
[21]   Zhang X., He M., and Zhang Y., 2012, "A review of research on the Kalina cycle," Renew. Sustain. Energy Rev., **16**(7), pp. 5309–5318.
[22]   AspenTech, 2013, "Aspen Plus" [Online]. Available: www.aspentech.com/products/aspen-plus.aspx. [Accessed: 30-Aug-2013].
[23]   Mathias P. M., Boston J. F., and Watanasiri S., 1984, "Effective utilization of equations of state for thermodynamic properties in process simulation," AIChE J., **30**(2), pp. 182–186.
[24]   Coastal Chemical Company, 2013, "HITEC Heat Transfer Salt" [Online]. Available: www.coal2nuclear.com/MSR - HITEC Heat Transfer Salt.pdf. [Accessed: 30-Aug-2013].
[25]   Yang Z., and Garimella S. V., 2010, "Thermal analysis of solar thermal energy storage in a molten-salt thermocline," Sol. Energy, **84**(6), pp. 974–985.
[26]   National Institute for Standards and Technology, 2013, "REFPROP MATLAB Interface" [Online]. Available: www.boulder.nist.gov/div838/theory/refprop/Frequently_asked_questions.htm#MatLabApplications. [Accessed: 30-Aug-2013].
[27]   SOLUCAR, 2006, "PS10: a 11.0-MWe Solar Tower Power Plant with Saturated Steam Receiver" [Online]. Available: www.upcomillas.es/catedras/crm/report05/Comunicaciones/Mesa IV/D. Valerio Fern%25C3%25A1ndez - Solucar 2.pdf. [Accessed: 30-Aug-2013].
[28]   Birnbaum J., Eck M., Fichtner M., Hirsch T., Lehmann D., and Zimmermann G., 2010, "A direct steam generation solar power plant with integrated thermal storage," J. Sol. Energy Eng., **132**(3), p. 031014.
[29]   Madaeni S. H., Sioshansi R., and Denholm P., 2012, "How thermal energy storage enhances the economic viability of concentrating solar power," Proc. IEEE, **100**(2), pp. 335–347.